 doi:10.20944/preprints202011.0210.v1

Article

Enhancing mechanical properties and biological performances of injectable bioactive glass by gelatin and chitosan for bone small defect repair

Mehri Sohrabi[1], Bijan Eftekhari Yekta[1,*], Hamidreza Rezaie[1], Mohammad Reza Naimi-Jamal[2], Ajay Kumar[3], Andrea Cochis[3], Marta Miola[4] and Lia Rimondini[3,*]

[1] School of Metallurgy & Materials Engineering, Iran University of Science and Technology, Tehran, Iran. sohrabi_m@metaleng.iust.ac.ir (M.S.); beftekhari@iust.ac.ir (B.E.Y.); hrezaie@iust.ac.ir (H.R.).
[2] Department of Chemistry Research laboratory of green organic synthesis and polymers, Iran University of Science and Technology, Tehran, Iran. naimi@iust.ac.ir (M.R.N.J.).
[3] Department of Health Sciences, Center for Translational Research on Autoimmune and Allergic Diseases–CAAD, University of Piemonte Orientale UPO, Novara, Italy. ajaykumar2420@gmail.com (A.K.); andrea.cochis@med.uniupo.it (A.C.); lia.rimondini@med.uniupo.it (L.R.).
[4] Department of Applied Science and Technology, Politecnico di Torino, Turin, Italy. marta.miola@polito.it (M.M.).

* *Correspondence*:
Prof. Bijan Eftekhari Yekta (B.E.Y)
Iran University of Science and Technology, Tehran, Iran
beftekhari@iust.ac.ir
Prof. Lia Rimondini (L.R.)
University of Piemonte Orientale UPO, Novara, Italy
lia.rimondini@med.uniupo.it

Abstract: Bioactive glass (BG) represents a promising biomaterial for bone healing; here injectable BG pastes biological properties were improved by 25 wt% gelatin or chitosan, as well as mechanical resistance was enhanced by adding 10 or 20 wt% 3-Glycidyloxypropyl trimethoxysilane (GPTMS) cross-linker. Composites exhibited bioactivity as apatite formation was observed by SEM and XRD after 14 days immersion in SBF; moreover, polymers did not enhance degradability as weight loss was >10% after 30 days in physiological conditions. BG-gelatin-20 wt% GPTMS composites demonstrated the highest compressive strength (4.8±0.5 MPa) in comparison with 100% BG control (1.9±0.1 MPa). Cytocompatibility was demonstrated towards human mesenchymal stem cells (hMSC), osteoblasts progenitors and endothelial cells. The presence of 20 wt% GPTMS conferred antibacterial properties thus inhibiting the joint pathogens *Staphylococcus aureus* and *Staphylococcus epidermidis* infection. Finally, hMSC osteogenesis was successfully supported in a 3D model as demonstrated by alkaline phosphatase release and osteogenic genes expression.

Keywords: bioactive glass; gelatin; chitosan; 3-Glycidyloxypropyl trimethoxysilane; bone.

 doi:10.20944/preprints202011.0210.v1

1. Introduction

The development of composites mimicking bone-like tissue in terms of physical, chemical and topographical properties represent a fascinating challenge for tissue engineering with the aim to improve tissue healing. Accordingly, bone-dedicated biomaterials have been developed in order to be cytocompatible, absorbable and anti-inflammatory as well they have been molded using various topography such as block, granule, porous and dense [1-5]. Between the large class of biomaterials aimed at bone repair, bioactive glass (BG) represents a very promising tool due to its ability to form apatite on the surface thus easily establish a chemical bond with the naïve bone tissue [6-8]. However, despite the BG demonstrated biocompatible, osteoconductive and osteointegrative behavior, its usage is limited in load-bearing sites. In fact, although BG holds high compressive strength, it is extremely brittle and does not withstand tensile and flexural loads [9-11]. Therefore, the use of polymers and cross-linkers in combination with BG to improve mechanical properties can be a suitable solution. In particular, the focus of this study was devoted to developing an easy-to-handle, injectable composite paste to fill small bone defects.

Due to the need of injectability, bone pastes are viscous solutions easy to be handled by clinicians to fill small defects but holding poor mechanical strengths; so, this defect open for the possibility that the paste does not support bone mechanical stress after injection thus making it necessary a new operation. To overcome this limitation, we hypothesized to exploiting the direct correlation between the mechanical properties and the composites structure; accordingly, the glycidyloxypropyl trimethoxysilane (GPTMS) was added as cross-linker to improve BG's mechanical strength. The hypothesized improvement is due to the crosslinking occurring between GPTMS and the paste components: in fact, the paste mechanical properties result as improved by the covalent bond between the epoxy groups in GPTMS and the NH_3^+ groups in chitosan and gelatin, and by the ionic bonding with the bioactive glass powder. Previous literature already demonstrated the suitability of such strategy: for example, Kuo and Ma showed that by increasing the sodium concentration from 1 w/v% to 2 w/v%, the compressive modulus of alginate hydrogels increased from 5 KPa to 17 KPa [12]. In another study, Ishihara et al. showed that chitosan can be induced to reach the gelation phase and prevent bleeding in less than 1 minute by photo-crosslinking thus accelerating the wound healing [13].

Bone tissue is a mixture of mineral and organic phases: so, it can be considered as a kind of composite from the chemical point of view. BG is a very promising biomaterial for bone healing just why it can precisely mimic the chemical structure of the naïve tissue. Here, a combination between BG and polymers has been hypothesize also to improve the biological performances of the BG thanks to the biopolymers ability to resemble the extracellular matrix (ECM) components thus making the composites as more "friendly" for cells [14]. In particular, chitosan and gelatin have been selected due to their proved cytocompatibility with cells.

Chitosan is a biopolymer derived from chitin diacetylation and because of its antibacterial, biocompatible and biodegradable properties, it is a good candidate for biomedical applications [15-18]. The reason why chitosan can improve cells adhesion and proliferation is due to its similarity with glycosaminoglycans which are the main components of bone and cartilage ECM [19-21].

Gelatin is the second polymer here applied; its ability in promoting tissue repair is due to the collagen-like structure which stimulates cells adhesion providing a temporary substrate with high similarity with the cells ECM [22]. Gelatin-polysaccharide hybrids have different applications in biomedical such as bioprinting, gene delivery, drug delivery, wound healing and antimicrobial formulations [23,24]. The gelatin-polysaccharide hybrid can absorb water up to 100 times in comparison with its dry weight thus providing suitable conditions for cell recruitment, adhesion, spread and proliferation [25, 26]. In fact, the polysaccharide component can enhance the strength of the scaffold while the Arg-Gly-Asp (RGD)-like sequence holds the ability to increase migration and cell adhesion [27,28].

Those biopolymers can be considered as very promising for tissue engineering purposes as demonstrated from the variety of gelatin-chitosan hydrogel applications such as skin, cartilage and bone repair [29-31]. In previous studies, the effect of bioactive glass on PCL/chitosan nanofibers for

Preprints (www.preprints.org) | NOT PEER-REVIEWED | Posted: 5 November 2020 doi:10.20944/preprints202011.0210.v1

bone healing was investigated by Shaluman at al. [32]. In another study, Gentil et al. [33] found that bioactive glass SiO_2-P_2O_5-CaO-MgO-Na_2O-K_2O enriched with 70 wt% gelatin-chitosan exhibited great bioactivity. Bioactivity and mechanical properties of 55S bioactive glass- chitosan composite and the influence of 55S bioactive glass on the chemical properties of gelatin-chitosan scaffolds were investigated by Peter et al. [34,35]. The effect of 45S5 bioactive glass on mesenchymal stem cell activity in chitosan-gelatin scaffolds was investigated by Xynos et al. In other study, Bielby et al. [36] and Li et al. [37] showed that 58S bioactive glass 60 mol% SiO2-33 mol% CaO-7 mol% P_2O_5 was biocompatible, bioactive and biodegradable and thus suitable for bone repair applications. Maji et al. [38] prepared the 58S bioactive glass (57.44 mol%SiO_2- 35.42 mol% CaO- 7.15 mol% P_2O_5)-gelatin-chitosan scaffold by the Freeze-Drying method and investigated the effect of adding bioactive glass to this scaffold on the mechanical properties and cellular activity of mesenchymal stem cell (hMSC).

Based on these premises, in this study we investigated the effects of adding chitosan and gelatin polymers on composite based on 64S bioactive glass. The composites were compared to the 100% BG control in terms of mechanical properties, degradation, apatite formation, cytocompatibility, infection prevention and ability to support hMSC osteogenesis in a 3D-like model.

2. Materials and Methods

2.1 Bioactive glass (BG) and BG-polymers composites preparation

Chitosan, gelatin and 3-Glycidyloxypropyl trimethoxysilane (GPTMS) were purchased from Sigma-Aldrich. Triethyl phosphate, tetraethyl orthosilicate, nitric acid solution, calcium nitrate tetrahydrate, magnesium nitrate and ammonia solution were purchased from Merck. Bioactive glass (BG) with the composition of SiO_2 64, CaO 27, MgO 4 and P_2O_5 5 mol% was prepared by sol-gel method as shown in the Figure 1A according to previous literature [39,40].

The formed gel was incubated in the air dryer at 70 °C for 2 days and then further dried for 2 days in the oven at 120 °C. Then, to remove organic materials and nitrates, the gel was placed at 700 °C for 3 hours. In the next step, the bioactive glass powder was mechanically grounded in agitation (400 rpm) for 2 hours. For the preparation of gelatin-chitosan-bioactive glass (Gel-Cn-BG) biocomposites, 3 wt% polymer solutions gelatin (water soluble) and chitosan (soluble in acetic acid 1M) were prepared. The composites were prepared using different BG powder/polymers solutions and GPTMS (10 or 20 wt% of dried polymers weight) ratios as detailed in Table 1.

Table 1. Bioactive glass (BG) and BG-polymers chitosan (Cn) or gelatin (Gel) composites settlement.

Cn[1]	Gel[1]	BG[1]	GPTMS[2]	Specimen code	Description
0	0	0.25	0	Control	Mixed with distilled water
1	0	0.25	10	A	-
1	0	0.25	20	B	-
0	1	0.25	10	C	-
0	1	0.25	20	D	-
0.5	0.5	0.25	10	E	-
0.5	0.5	0.25	20	F	-

[1]*All values for polymer solutions and bioactive glass powder are expressed in grams.*

[2]*All values for GPTMS are expressed as wt%.*

According to Table 1, the materials were mixed and stirred for 30 minutes (room temperature). The obtained pastes (BG-Gel-Cn-GPTMS) were placed into cylindrical PTFE mold to obtain 1 x 1 cm disks and then placed at 37 °C to fully dry as schematized in Figure 1B.

Preprints (www.preprints.org) | NOT PEER-REVIEWED | Posted: 5 November 2020 doi:10.20944/preprints202011.0210.v1

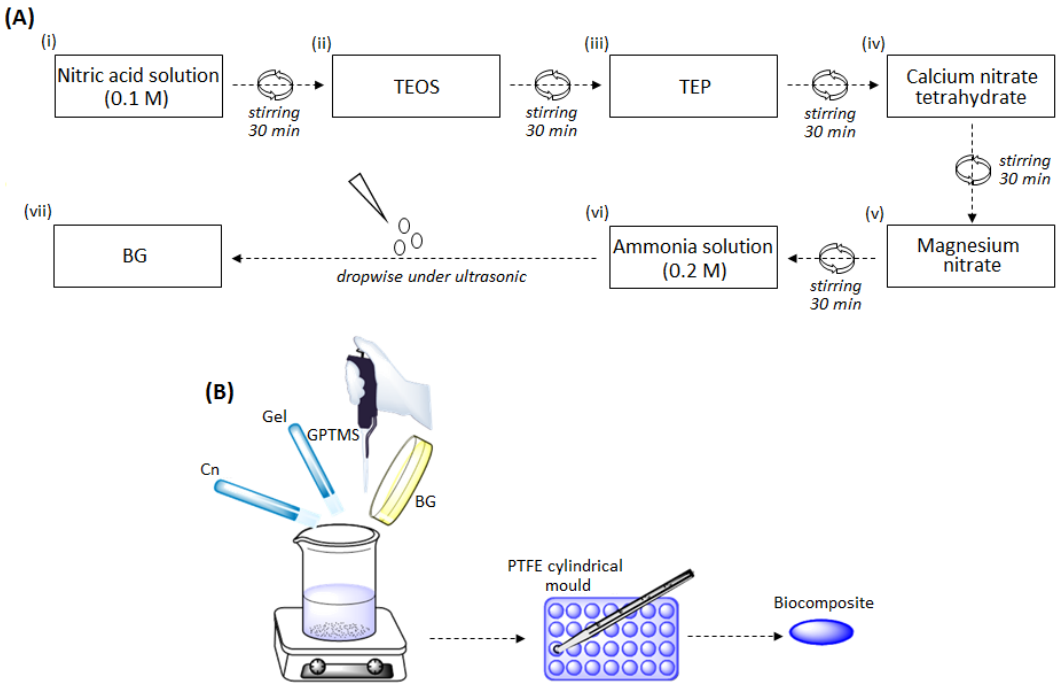

Figure 1. *Schematization of the sol-gel process (A) and of the composites preparation method (B).*

2.2 Physical-chemical Characterization

2.2.1 In vitro bioactivity test: X-Ray Diffraction (XRD) Analysis

To evaluate composites' bioactivity, the formation of apatite crystal was evaluated after 14 days immersion in body simulated fluid (SBF) at 37 °C, 7.4 pH, following the Kokubo' methods [41] using a ratio of 1 g/100 ml. At the end of the time-point, the composites were removed from the SBF solution, washed twice with bi-distilled water to remove any residual salts and stored at 37 °C to air-dry. The phase composition of the powdered composites, before and after SBF immersion, was measured by means of XRD with Cu-Kα radiation, wavelength of 1.54050 Å (Dron 8, Bourevestink, Russia) at 40 kV, 40 mA, step size of 0.04 and a count time of 2 s/step.

2.2.2 Mechanical strength

To estimate the mechanical compressive strength of composites, the universal testing machine STM 120 (from Santam Co.) was used. Briefly, composites were placed at room temperature in the machine and imposed to an increasing compressive force with crosshead speed of 0.01 mm/sec.

2.2.3 Scanning Electron Microscope (SEM) Analysis

The morphology of the composites before and after 14 days immersion in SBF solution was visually evaluated by SEM (TEScan, VeGa II, Czech).

2.2.4 Degradation

To evaluate specimens' degradation and anti-washout properties, composites, produced as described in paragraph 2.1, were individually weighted (=day 0) and immersed at 37 °C in SBF for 1, 7, 21 and 30 days. At each time points, the weight was recorded and compared to day 0 value; so, results were expressed as % of the day 0 value that was considered as 100% [42, 43].

Preprints (www.preprints.org) | NOT PEER-REVIEWED | Posted: 5 November 2020 doi:10.20944/preprints202011.0210.v1

2.3 Composites' Biological characterization

Biological characterizations were performed using composites disks (1 cm high x 1 cm diameter). Prior to experiments specimens were sterilized under class II safety cabinet by UV light for 1 hours (30 minutes/side) and stored at room temperature in sterile Petri dishes.

2.3.1 Direct cytocompatibility evaluation

2.3.1.1 Cells cultivation

Cells representative for the bone healing process after composites implantation were tested. Accordingly, human mesenchymal stem cells (hMSCs), human primary osteoblasts progenitors and human endothelial cells were directly cultivated in contact with control and test composites.

Human mesenchymal stem cells (hMSC) were obtained from Merck (PromoCell C-12974) and cultivated in low-glucose Dulbecco's modified Eagle Medium (DMEM, Merck) supplemented with 15% fetal bovine serum (FBS, Merck) and 1% antibiotics (penicillin/streptomycin, Merck) at 37 °C, 5% CO_2 atmosphere. Human primary osteoblasts progenitors (hFOB 1.19 CRL-11372) were purchased from the American Type Culture Collection (ATCC, Manassas, USA) and cultivated in MEM/F12 mix medium (50:50, from Sigma) 10% fetal bovine serum (FBS, from Sigma) 1% antibiotics and 3 mg/ml neomycin (G418 salt, Sigma) at 34 °C, 5% CO_2 atmosphere. Human endothelial cells (EA.hy926, CRL-2922) were purchased from ATCC and cultivated in high-glucose Dulbecco's modified Eagle Medium (DMEM, Sigma-Aldrich) supplemented with 10% fetal bovine serum (FBS, Sigma) and 1% antibiotics (penicillin/streptomycin) at 37 °C, 5% CO_2 atmosphere. Cells were cultivated until 80-90% confluence, detached by trypsin-EDTA solution, harvested and used for experiments.

2.3.1.2 Direct evaluation

Cells were directly seeded onto specimens' surface in a defined concentration ($1x10^4$ cells/specimen), allowed to adhere for 2 hours and then submerged with 1 ml of each specific medium. Cells-seeded composites were cultivated for 1 and 3 days. At each time points, the viability of the cells in direct contact with specimens was evaluated by the metabolic colorimetric Alamar blue assay (Alamar Blue™, from Life Technologies) following Manufacturer's instructions. Briefly, supernatants were removed from each well containing cells and replaced with Alamar blue solution (10% v/v in fresh medium). Plates were incubated in the dark for 4 hours and then 100 µl were removed, spotted into a new black 96-well plate and fluorescence signals were evaluated with a spectrophotometer (Spark®, Tecan Trading AG, CH) using the following set-up: fluorescence excitation wavelength 570 nm, fluorescence emission reading 590 nm. Specimens made of 100% BG were used as control and considered as 100% viability; accordingly, test specimens' values were normalized towards controls.

2.3.2 Composites' Antibacterial properties

2.3.2.1 Strains growth conditions

Two orthopedic infections-related strains bacteria were purchased from ATCC: the Gram-positive Staphylococcus aureus (SA, ATCC 43300) and Staphylococcus epidermidis (SE, ATCC 14990) were used to assay specimens' antibacterial properties [44]. Bacteria were cultivated onto Trypticase Soy Agar (TSA, Sigma-Aldrich) and incubated at 37 °C until round single colonies were formed; then, 2-3 colonies were collected and spotted into 30 ml of Luria Bertani broth (LB, Merck). Broth cultures were incubated overnight at 37°C in agitation (120 rpm in an orbital shaker). Lastly, a fresh culture was prepared prior to each experiment; bacteria concentration was adjusted until $1x10^3$ cells/ml by diluting in fresh media until optical density of 0.00001 at 600 nm was reached as determined by

Preprints (www.preprints.org) | NOT PEER-REVIEWED | Posted: 5 November 2020 doi:10.20944/preprints202011.0210.v1

spectrophotometer (Spark, Tecan). Pure medium was used as blank to normalize bacteria optical density.

2.3.2.2 Biofilm metabolic activity

Sterile specimens were gently moved into a 24 multiwell plate by sterile tweezers avoiding any damages. Each specimen was submerged with 1 ml of the $1x10^3$ cells/ml broth culture prepared as prior described in paragraph 2.3.2.1; plate was incubated for 90 minutes in agitation (120 rpm) at 37 °C to allows the separation between adherent biofilm cells and not-adherent floating planktonic cells (separation phase) [45, 46]. Afterwards, supernatants containing planktonic cells were removed and replaced with 1 ml of fresh media to cultivate surface-adhered biofilm cells (growth phase) [45, 46]. Biofilm were grown at 37 °C for 1 and 3 days prior to evaluations. At each time-point, specimens were gently washed 2 times with PBS to remove non-adherent cells and then moved to a new 24 multiwell plate where bacteria metabolic activity was evaluated by the Alamar blue assay as prior described for cells metabolic activity evaluation. 100% BG were used as control and considered 100% viability while test values normalized towards them.

2.4 Composites' Pro-osteogenic properties

2.4.1 3D bone-like model

After the evaluation of specimens' cytocompatibility and antibacterial activity, the following composites were selected as the most promising and used for further analysis: B and D (according to Table 1). Accordingly, they were used to test cells ability to grow within specimens' pores simulating a 3D matrix [47, 48]. First, hMSC were mixed in a defined number ($1x10^6$) into 50 µl of a liquid collagen matrix (PureCol™ EZ Gel solution, from Sigma); then, the collagen loading cells were slowly dropwise into the composites at room temperature (liquid phase) to completely fill their pores. Afterwards, composites filled with cells were moved into the incubator at 37 °C to allows collagen gelation phase to act as temporary support for cells growing in a 3D matrix. Finally, composites were submerged with 1 ml of fresh medium and cultivated for 7 and 15 days. At each time-point cells metabolism was evaluated by the Alamar blue assay as previously described. 100% BG were used as control and considered 100% viability while test values normalized towards them.

2.4.2 Alkaline phosphatase (ALP) activity

To verify the BG pro-osteogenic effect and to evaluate a possible improvement coming from the polymers adjunct, the 3D model described in 2.4.1 was cultivated for 3-7-11-15 days in the presence of maintenance medium (intended as low-glucose DMEM 15% FBS 1% antibiotics) thus avoiding the use of any osteogenic biochemical stimulation. At each time point supernatants were collected and the Alkaline phosphatase (ALP) activity was measured to evaluate cells maturation towards bone-like lineage using a colorimetric assay (ab83369, from AbCam, UK). Briefly, 80 µl of supernatants were collected from each sample and mixed with 50 µl of the pNPP solution and 10 µl of the ALP enzyme (provided from the kit). After 60 minutes incubation, the reaction was stopped and the optical density was measured by spectrophotometer (Spark®, Tecan Trading AG, CH) using a 405 nm wavelength.

2.4.3 Gene expression

After 15 days cultivation in maintenance medium as prior described in 2.4.2, the expression of osteogenic genes collagen I (COL 1), alkaline phosphatase (ALP) and osteopontin (OPN) [49] was

Preprints (www.preprints.org) | NOT PEER-REVIEWED | Posted: 5 November 2020 doi:10.20944/preprints202011.0210.v1

assessed by means of real-time PCR. Briefly, specimens were manually fragmented allowing cells homogenization by TRIzol reagent (Sigma). Then, RNA was isolated by isopropanol precipitation and reverse transcribed using a TaqMan kit (from Applied Biosystems, USA). For real-time PCR TaqMan Gene Expression Assays (Applied Biosystems) were used on a GeneAmp 7500 Real Time PCR System (Applied Biosystems) using the 18S rRNA (Applied Biosystems 4310893E) as housekeeping gene. Finally, selected genes expression was normalized towards the starting expression level (intended as the seeding day expression) by the $^{\Delta\Delta}$Ct method.

2.4.4 Morphological evaluation

Cells morphology was visually checked after 7- and 15-days culturing by means of scanning electron microscopy (SEM). Briefly, cells were fixed with 4% formaldehyde for 12 hours, dehydrated by alcohol scale (50%, 70%, 90% and 100%, 3 hours each) and finally treated with hexamethyldisilazane (from Alfa Aesar) to give 3D shape to the cells. Then, specimens were mounted onto aluminum stubs using conductive carbon tape to undergo surface metallization by means of a chromium layer and observed with a SEM-EDS JEOL NEOSCOPE JCM 6000 PLUS using secondary electrons (Nikon Instrument S.p.A., Firenze, Italy).

2.5 Statistical analysis of data

Experiments were performed using 6 replicates. Normal distribution and homoscedasticity were tested with Wilk-Shapiro's and Levene's test respectively. Samples were statistically compared by the SPSS software (v25, IBM) using the one-way ANOVA test and the Tukey's post-hoc analysis. Results were considered as significant for $p<0.05$.

3. Results and Discussion

3.1 Composites physical-chemical characterization

3.1.1 XRD and SEM analysis

The morphology and the phase analysis of composites before and after immersion in SBF solution was evaluated by XRD and SEM, respectively. Results are reported in Figure 2A-B.

XRD spectrum (Fig. 2A) of composites before SBF treatment showed the presence of broad amorphous halo, indicating that the composites were amorphous prior to SBF immersion (indicated as day 0). Conversely, after the immersion of the composites in SBF solution for 14 days, the crystalline peak of hydroxyl carbonate (code: 024240) apatite was observed at about $2\theta=32°$ [39,40], in addition to the amorphous halo. The formation of hydroxyapatite layer in these composites is due to the presence of the bioactive glass (BG): in fact, apatite formation mechanism is based on BG components leading to the subsequent calcium phosphate deposition [50,51]. Due to the BG surface reactivity, Ca^{2+}, PO_4^{3-} and Mg^{2+} ions are replaced by H^+ ions in the SBF solution thus forming $Si(OH)_4$. Then, with increasing dissolution, a silica-rich layer was formed on the surface of BG; then, PO_4^{3-} and Ca^{2+} ions migrated through the SBF solution forming an amorphous calcium phosphate layer on the top of glass-rich silica layer. The crystalline layer of hydroxyl carbonate apatite was then formed by the participation of OH^- and CO_3^{2-} ions in the SBF solution [52]. The presence of the polymers (chitosan or gelatin) improved the bioactivity of the BG thus enhancing the formation of apatite crystals. In fact, the negatively charged functional groups (COO^-) of gelatin and chitosan were able to absorb calcium and phosphorus ions by electrostatic forces, thus leading to an increased apatite formation on the composite surface as previously observed by others [53,54]. Finally, SEM images (Fig. 2B) offered a visual confirmation of the apatite formation onto composite surface after 14 days in SBF immersion (highlighted by the red arrows).

Preprints (www.preprints.org) | NOT PEER-REVIEWED | Posted: 5 November 2020 doi:10.20944/preprints202011.0210.v1

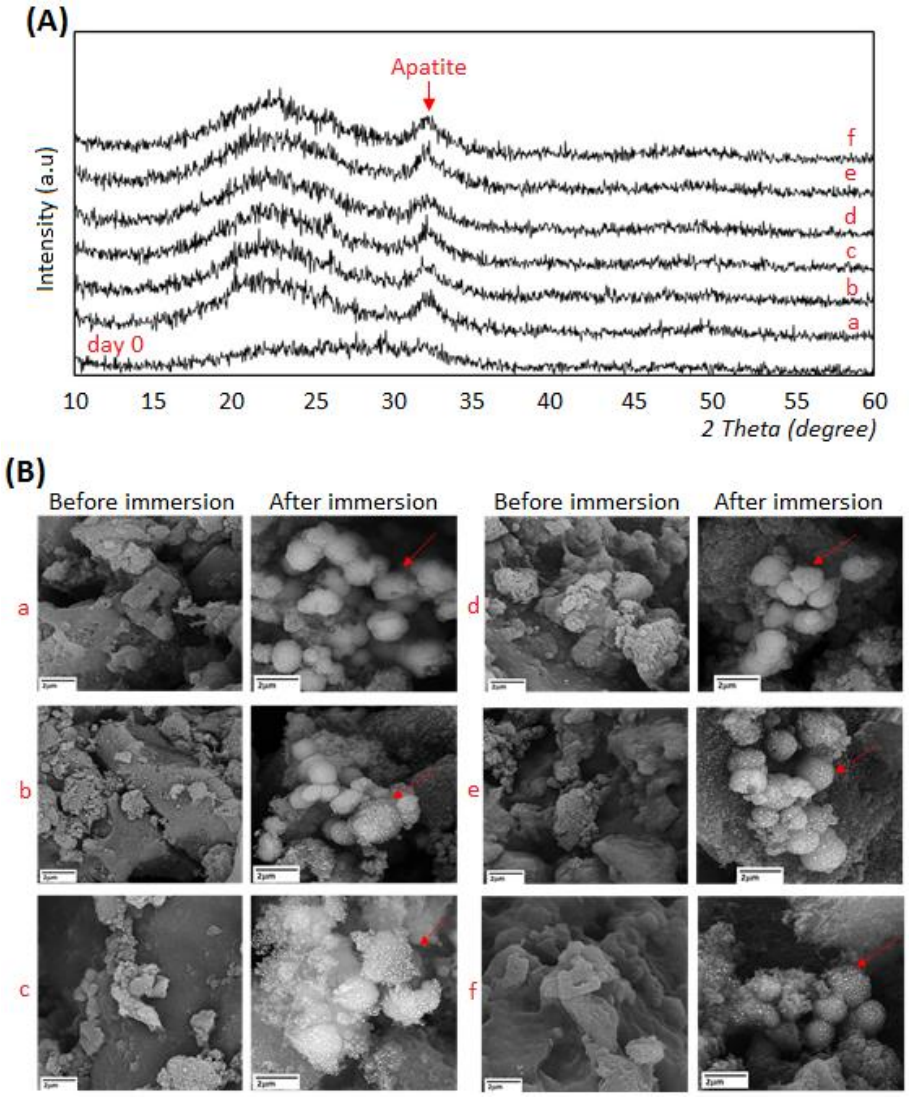

***Figure 2**. XRD spectra (A, upper panel) and SEM images (B, lower panel) of composites before (=day 0) and after immersion in SBF solution for 14 days. Apatite formation was confirmed for all the tested specimens by both XRD that showed typical apatite peaks and SEM which images demonstrated the presence of crystals aggregates (indicated by the red arrows). SEM magnifications: 15000x (before immersion) and 20000x (after immersion). A-f refer to the composites as detailed in Table 1.*

3.1.2 Mechanical strength

Compressive strength was applied onto control (100% BG) and GPTMS cross-linked composited to verify whether the presence of a cross-linker and the addition of polymers resulted as beneficial in relation to the ability to support mechanical stress. Results are summarized in Table 2. In general, results revealed that the chemical bond between GPTMS and other composite components reduces the brittleness and increased mechanical strength. In fact, specimens' carrying 20 wt% GPTMS (named as B-D-F) reported the highest values if compared to the control (100% BG) and the same compositions but cross-linked with 10 wt% (intended as: a *vs* b; c *vs* d; e *vs* f). In particular, the composites made of BG-gelatin-GPTMS wt% 20 (named as D) reported the best mechanical resistance (4.8±0.5 MPa). The key-role of the cross-linker was confirmed by the fact that values were superior when GPTMS was used at 20 wt% in comparison to 10 wt%, thus confirming a dose-dependent effect. The enhanced mechanical properties are due to the presence and the amount of both the cross-liker and the polymers; in fact, GPTMS have the ability to bond with the amino groups of chitosan and

Preprints (www.preprints.org) | NOT PEER-REVIEWED | Posted: 5 November 2020 doi:10.20944/preprints202011.0210.v1

gelatin [55,56], thus forming strong bonds conferring higher stability to the composites. Moreover, also the silanol groups in the GPTMS can bind with chitosan and gelatin so adding further stability to the composites' structure [57]. Such results seem to be in line with previous literature; as an example, Ravarian et al [58] demonstrated that the use of GPTMS in combination with chitosan and BG was effective in improving the composites mechanical properties. Accordingly, it can be speculated that the parallel increasing of GPTMS wt% and mechanical properties is probably due to the presence of more covalent bonds between chitosan, gelatin and bioactive glass.

Table 2. Composites' mechanical strength evaluation.

Specimen	Control	a	b	c	d	e	f
Value[1]	1.9±0.1	1.8±0.5	2.5±0.2	3.7±0.3	4.8±0.5	2.8±0.3	3.2±0.2

[1] *Results are expressed in MPa.*

3.1.3 Degradation

Ideal composites aimed at small bone defects healing should such as injectable pastes should be bioresorbable and biodegradable, but at the same time they must be able to withstand in the injured site until the formation of the new tissue. Accordingly, the degradation of the composites was here tested over a 30 days period in physiological conditions (SBF immersion, 37 °C) by means of specimens' weight loss in comparison with day 0 (intended as prior to SBF immersion) values that were considered as 100%. Results are reported in Figure 3.

In general, all composites demonstrated to well tolerate degradation up to day 21 (>95% in comparison to the day of weight). Conversely, they showed a significant degradation rate after 30 days with a weight loss between 16% and 10%. However, this can be considered as an acceptable time for naïve bone healing so it can be hypothesized that the newly formed tissue can replace the degrading composites after 30 days [59].

The polymers adjunct enhanced composites' strength towards degradation in comparison to BG controls thus confirming their pivotal role for the composites stability as previously observed for the mechanical properties' evaluation. In fact, chitosan and gelatin can swell the composite by absorbing water in their structure, then swelling increases the pores size and porosity, thereby helping to supply nutrients and oxygen to the composite network. This behaviour can be of crucial importance in the healing process when cells penetrate the composite pores with the aim to repopulate the injured site. A similar trend was observed by Peter et al. [34]; they showed that the degradation of chitosan-bioactive glass scaffolds was significantly less than chitosan scaffolds thanks to a mutual support. In fact, chitosan degradation is normally speed up in acidic environment but thanks to the release of alkali groups of bioactive glass, the environment was neutralized, and the scaffold degradation decreased [34]. Therefore, while chitosan improved the stability of the BG structure, the BG itself modified the pH of the environment thus preserving the polymer from a fast degradation.

Preprints (www.preprints.org) | NOT PEER-REVIEWED | Posted: 5 November 2020 doi:10.20944/preprints202011.0210.v1

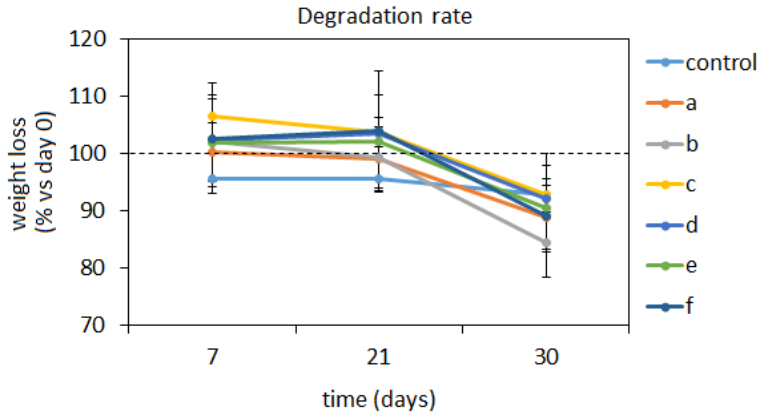

***Figure 3**. Composites degradation rate over time under SBF immersion at 37 °C. Results are expressed as % of the weight recorded at day 0 prior to immersion considered as 100%.*

3.2 Composites biological characterization

3.2.1 Composites cytocompatibility

As previously discussed in the Introduction section, the here developed composites are aimed at injectable pastes for bone small defects as temporary substitutes supporting tissue self-healing. Accordingly, materials' cytocompatibility has been *in vitro* assayed towards mesenchymal stem (hMSC) cells and foetal osteoblasts progenitors (hFOB): those particular cell lines were selected as representative for cells deputed for the tissue self-healing as resident progenitor cells (hFOB) or recruited from the neighbourhood to migrate into the injured site (hMSC) [60]. Moreover, endothelial cells (EA.hy296) have been tested in direct contact with test composites too as the neo-vascularization of the healing tissue represents a crucial step for the recruitment of nutrients as well as for the biochemical crass-talk [61]. Results are reported in Figure 4A-C.

In general, test composites demonstrated to be more cells friendly in comparison with the 100% BG controls (that were considered as 100% viability) for all the tested cells lines by reporting values >100% (indicated by the dashed lines). In details, hMSC viability (Fig. 4A) was significant in comparison with control for composites d-e-f after 1 day in direct contact ($p<0.05$, indicated by *) as well as after 3 days ($p<0.05$, indicated by #). Osteoblasts progenitors hFOB (Fig. 4B) reported a significantly higher viability in comparison with controls after day 1 for a-c-d-e-f composites ($p<0.05$, indicated by *) but only for d after 3 days ($p<0.05$, indicated by #). Finally, endothelial EA.hy296 cells (Fig. 4C) showed a significant increase in terms of viability in comparison with control for b-c composites after 1 day ($p<0.05$, indicated by *) while a-b resulted significant after 3 days ($p<0.05$, indicated by #).

According to the obtained results, it can be speculated that the introduction of polymers (gelatin or chitosan) and GPTMS as cross-linker into BG did not caused any toxic effect towards the tested cell lines; moreover, some formulations reported significantly higher values thus suggesting to be helpful for cells adhesion and proliferation.

Those results are in line with previous literature showing that such polymers can improve osteogenesis for tissue engineering applications in combination with bioactive glasses. For example, Li et al. demonstrated that the use of gelatin doped with BMP-2 was successful in promoting osteogenesis in osteoporosis [62]. Moving towards chitosan, Mokhtari et al. used chitosan-58S bioactive glass nanocomposite coatings to improve the osteogenic properties of TiO_2 nanotubes [63]. The use of GPTMS did not introduced toxic compounds too; similarly, it was used to produce biocompatible tools such as pro-regenerative coatings for Ti alloys in combination with PFPE [64].

Finally, the presence of polymers and in particular of chitosan seems to promote the recruitment of endothelial cells thus probably favouring angiogenesis within scaffold pores; a similar effect was

Preprints (www.preprints.org) | NOT PEER-REVIEWED | Posted: 5 November 2020 doi:10.20944/preprints202011.0210.v1

observed by Najera-Romero et al. [65] heparinized chitosan/hydroxyapatite scaffolds promoted angiogenesis and ameliorated bone regeneration.

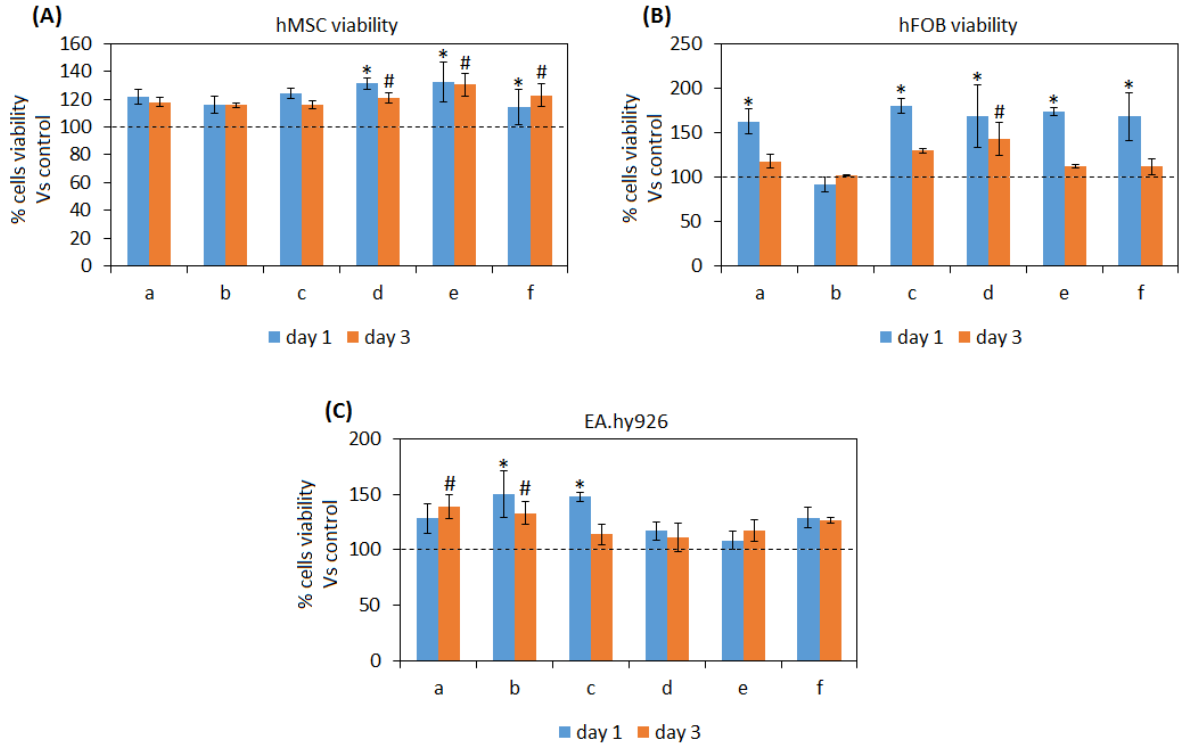

***Figure 4**. Composites' cytocompatibility towards mesenchymal stem cells (A), osteoblasts progenitors (B) and endothelial cells (C). All the composites formulations reported viability values >100% (indicated by the dashed lines) in comparison with 100% BG controls. Moreover, significant differences were noticed after 1 day ($p<0.05$, indicated by the *) or 3 days ($p<0.05$, indicated by the #) between composites as control. Bars represent means and standard deviations.*

3.2.2 Antibacterial properties

One of the most problematic aspect causing implant failure is represented by infections. Bacteria can enter the wound site due to the surgical procedures as well as by the injectable paste material itself if not properly sterilized [66]. Moreover, the increasing of drug-resistant pathogens strains is making infections treatment as more and more difficult due to strong resistance of such bacteria to the conventional antibiotic administration. So, it is of particular importance that injectable materials hold intrinsic properties to inhibit or at least to counteract bacteria colonization. Some of the here presented composites were hypothesized holding antibacterial properties due to the presence of anti-infective compounds such as chitosan [67] and GPTMS [68]. Accordingly, we test all the composites towards the ability to prevent the infection of *Staphylococcus aureus* (SA) and *Staphylococcus epidermidis* (SE), the two main pathogens involved in bone and joint infections. Results are reported in Figure 5.

As expected, results were strictly related to the composites formulation and in particular with the presence of chitosan. In fact, the best results were achieved by the composites b containing BG-chitosan-GPTMS wt20%: the biofilm contamination was comparable to the control materials for SA at both time points (Fig. 5A, $p>0.05$) while when SE infection was considered a significant reduction was observed after 3 days (Fig. 5B, $p<0.05$ vs controls, indicated by #). Chitosan antibacterial properties are well-know and it was demonstrated to be effective mostly towards Gram-positive bacteria but also to inhibit the biofilm formation of Gram-negative and some fungi [69]. Basically, the mechanism behind is due to the electrostatic interaction occurring between the positive charged groups of the chitosan and the negatively charged outer membrane of bacteria that causes an irreversible damage of the latter. In fact, chitosan structure is characterized by the presence of amino

Preprints (www.preprints.org) | NOT PEER-REVIEWED | Posted: 5 November 2020 doi:10.20944/preprints202011.0210.v1

groups that can bind with the lipopolysaccharides and the proteins that are found within the bacteria membrane (schematized in Fig. 5C); so, due to the above-mentioned interactions a change in the bacteria' membrane occurs leading to the formation of pores that causes intracellular components and nutrients leaking as well as membrane lysis [70].

Referring to other composites, no evidences of antibacterial activity were observed; on the opposite, for SA (Fig. 5A) a significant increase of biofilm metabolic activity was reported for specimens a-c-e after 1 ($p<0.05$, indicated by *) and 3 days ($p<0.05$, indicated by #) of infection. Therefore, despite a certain strain-dependent outcome and the promising results achieved from composites b, a more efficient strategy to improve antibacterial properties must be introduced as future perspective to face the problem related to the infections.

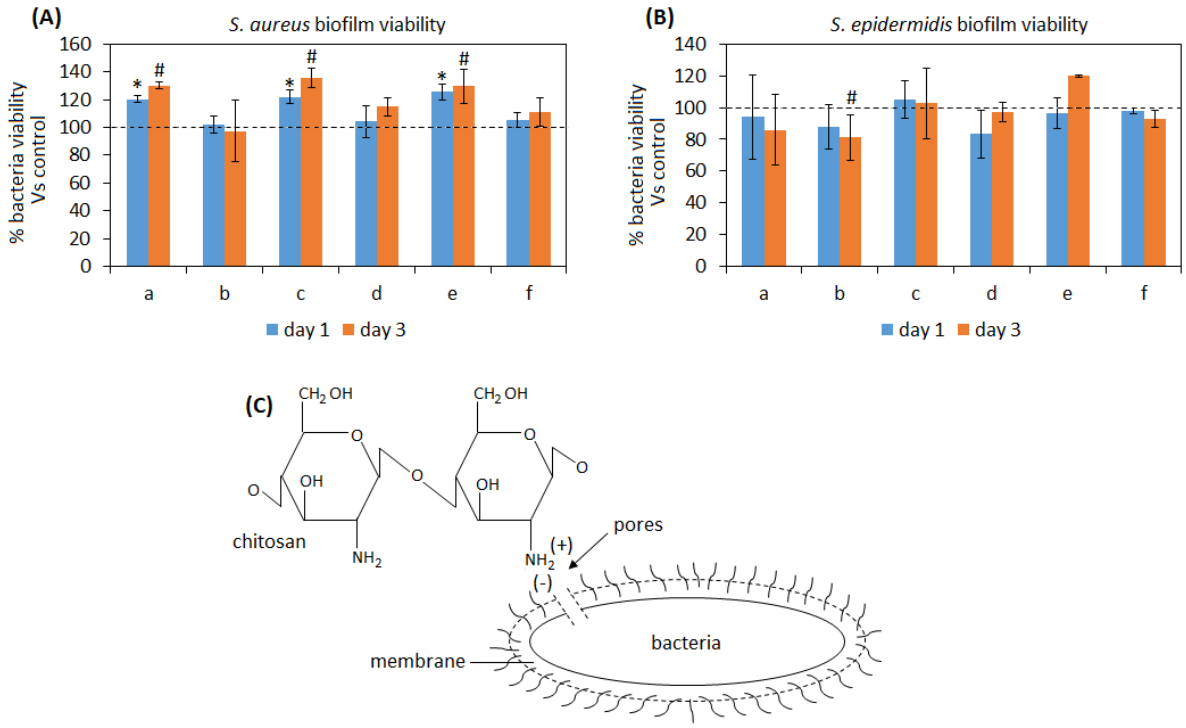

***Figure 5**. Composites' antibacterial properties towards Staphylococcus aureus (A, SA) and Staphylococcus epidermidis (B, SE). Only the composites b (BG-chitosan-GPTMS wt20%) were successful in counteracting SA biofilm and to significantly reduce SE one after 3 days in comparison with controls ($p<0.05$, indicated by #) due to chitosan properties as schematized in (C). Bars represent means and standard deviations.*

3.2.3 Osteogenic properties

After cytocompatibility and antibacterial evaluations the composites b and d were selected for osteogenic properties assays due to the high affinity with stem cells and osteoblasts progenitors (the main populations involved in the self-healing process) and due to the ability to counteract infections of the joint pathogens SA and SE here tested. Moreover, they are representative for compositions holding or chitosan (b) or gelatin (d) in combination with BG and GPTMS (wt20%) in order to better understand their role in promoting osteogenesis. Accordingly, mesenchymal stem cells (hMSC) were seeded into the pores of the composites and maintained in conservative medium (DMEM 15% FBS 1% antibiotics); the use of osteogenic chemicals such as dexamethasone and β-glycerophosphate was voluntarily prevented in order to exploit BG' bioactivity [49] and to evaluate the possible contribution of the polymers. Results are summarized in Figure 6.

Firstly, to confirm cytocompatibility results previously obtained by the cells monolayer experiments (showed in Fig 4A), the Alamar blue assay was used to check cells' metabolic activity over the 15 days planned for the osteogenic evaluation. As reported in Figure 6A, the use of polymers improved cells metabolism at each time-points even if not in a significant manner ($p>0.05$ vs control), thus

 doi:10.20944/preprints202011.0210.v1

confirming composites' cytocompatibility. Prior to run PCR to check osteogenic genes expression at day 15, the alkaline phosphatase (ALP) activity was measured in the supernatants after each medium change at 3-7-15 days as a marker of the osteogenic-like phenotype differentiation (Fig. 6B); as reported in Figure 6B, similar results between controls and composites were obtained after 3 and 7 days (Fig. 6B, $p>0.05$) but at day 15 cultivation a trend inversion was observed for specimens d, thus suggesting a possible role for gelatin in better support osteogenesis in comparison with both controls and chitosan-doped specimens (Fig. 6B, $p<0.05$, indicated by *). From this point of view, a large literature reported of a significant contribution from gelatin in enhancing pro-osteointegrative properties; for example, Lin et al, developed gelatin-based electrospun fibrous scaffolds with enhanced ability to promote hMSC osteogenic differentiation [71]. Similarly, Wu et al. reported how the gelatin introduction into calcium silicate cements improved mechanical properties and stem cells osteogenic response [72]. A possible explanation of the gelatin contribution comes from Ren et al [73] which showed how it can ameliorate wettability thus facilitating cells uptake of nutrients and chemical from the environment.

The hMSC osteogenic differentiation was checked by gene expression after 15 days cultivation by evaluating the osteogenic genes collagen type I (COL 1), alkaline phosphatase (ALP) and osteopontin (OPN). The 100% BG was considered as control due to the previously demonstrated evidence that its chemical composition is sufficient to directly promote osteogenic differentiation of mesenchymal stem cells [74,75] without the need of external stimulation useful to undergo other differentiation [75]. As reported by Fig. 6C, a similar gene expression pattern was found, thus demonstrating that the cells seeded within composites pores underwent osteogenic differentiation in a similar manner of the BG controls. This is a confirmation that the presence of polymers did not interfere with the chemical stimulation released from the BG that stimulate cells to differentiate towards bone phenotype. As prior observed for ALP activity released in the supernatant, samples d reported the highest genes fold increase expression in comparison to day 0, but results were not significant if compared to controls or samples b ($p>0.05$).

Finally, SEM images (Fig. 6D) confirmed that cells were correctly seeded into the composites' pores interacting with surrounding environment and that they displayed the stellate morphology that is typical of the mature osteoblasts, thus giving a visual confirmation of the bone-like differentiation occurring due to composites' pro-osteogenic activity.

Preprints (www.preprints.org) | NOT PEER-REVIEWED | Posted: 5 November 2020 doi:10.20944/preprints202011.0210.v1

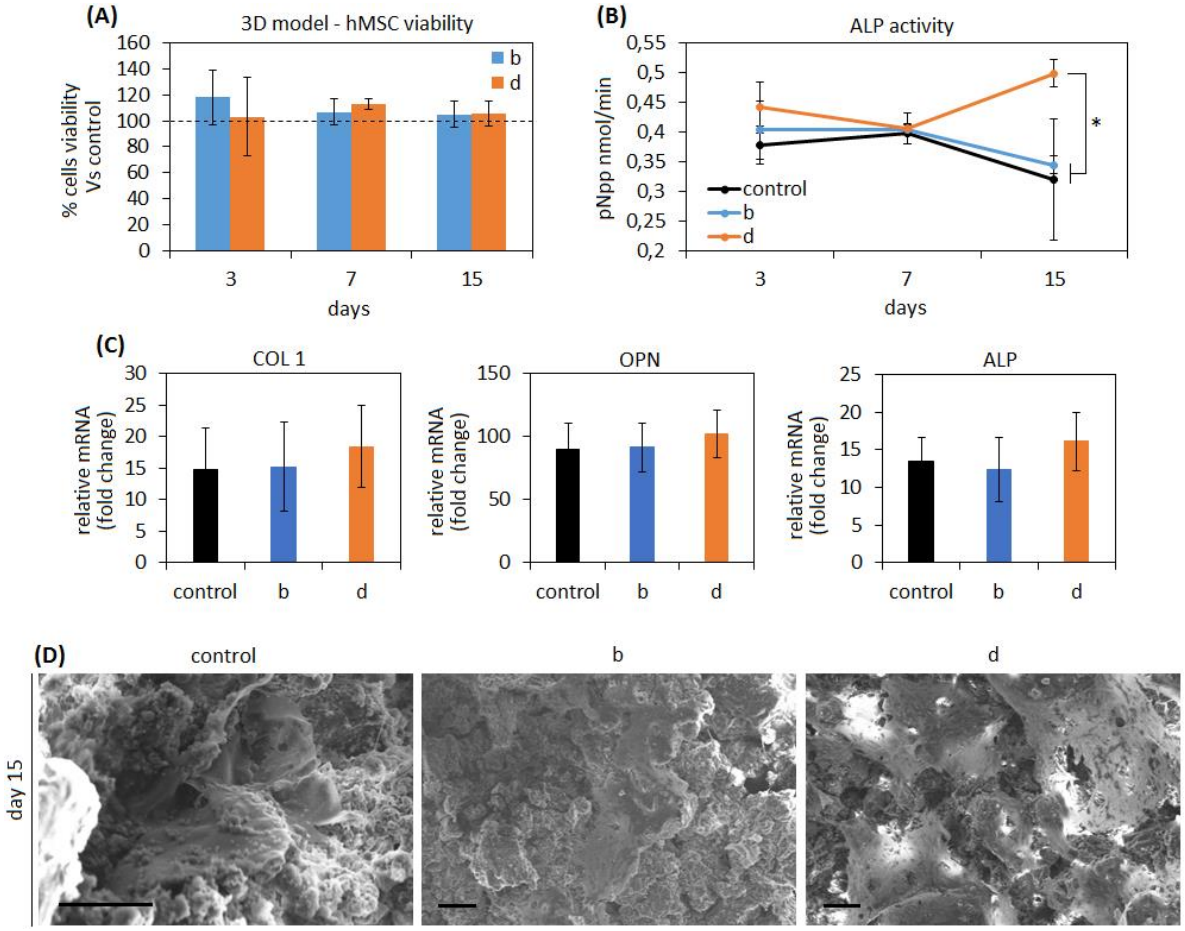

***Figure 6**. Osteogenic properties. Composites results as cytocompatible for pores 3D seeding (A) as well as they successfully supported hMSC osteogenic differentiation that was verified by alkaline phosphatase (ALP, B) increasing release in the medium and osteogenic genes collagen 1 (COL 1), osteopontin (OPN) and ALP expression (C). Finally, SEM images confirmed that cells grown within pores reached the osteoblast-like stellate morphology after 15 days cultivation. SEM images: bar scale=10μm.*

4. Conclusions

In order to ameliorate injectable pastes for small bone defects mechanical properties and biological performances, chitosan and gelatin were successfully coupled with bioactive glass using GPTMS as cross-linker. The composites demonstrated a bioactive behaviour and superior mechanical resistance towards compressive stress than pure glass as well as they improved the metabolic activity of cells deputed to undergo the tissue self-healing. Moreover, composites supported stem cells osteogenic differentiation in a 3D model avoiding the use of biochemical factors thus confirming a strong bioactivity. However, composites demonstrated to hold poor antibacterial properties thus failing in reducing pathogens infection; from this point of view, more efforts should be put in the future to confer intrinsic antibacterial properties in order to prevent infections.

Author Contributions: methodology, data curation and writing—original draft preparation: M.S., H.R., M.R.N.J., A.K., A.C., M.M.; writing—review and editing, supervision and project administration: L.R. and B.E.Y. All authors have read and agreed to the published version of the manuscript.

Conflicts of Interest: The authors declare no conflict of interest.

References

1. Nabiyouni, M.; Brückner, T.; Zhou, H.; Gbureck, U.; Bhaduri, S. B. Magnesium-based bioceramics in orthopedic applications. Acta Biomater **2018,** *66*, 23-43. DOI: 10.1016/j.actbio.2017.11.033
2. Rahaman, M. N.; Day, D. E.; Bal, B. S.; Fu, Q.; Jung, S. B.; Bonewald, L. F.; Tomsia, A. P. Bioactive glass in tissue engineering. Acta Biomater **2011,** *7* (6), 2355-2373. DOI: 10.1016/j.actbio.2011.03.016
3. Barrere, F.; Mahmood, T.; De Groot, K.; Van Blitterswijk, C..A. Advanced biomaterials for skeletal tissue regeneration: Instructive and smart functions. Mater. Sci. Eng. R **2008,** *59* (1-6), 38-71. DOI: 10.1016/j.mser.2007.12.001
4. Bohner, M. Resorbable biomaterials as bone graft substitutes. Mater. Today **2010,** *13* (1-2), 24-30. DOI: 10.1016/S1369-7021(10)70014-6
5. Wang, W.; Yeung, K. W. Bone grafts and biomaterials substitutes for bone defect repair: A review. Bioact. Mater **2017,** *2* (4), 224-247. DOI: 10.1016/j.bioactmat.2017.05.007
6. Minouei, H.; Fathi, M.; Meratian, M.; Ghazvinizadeh, H. Engineering, Heat treatment of cobalt-base alloy surgical implants with hydroxyapatite-bioglass for surface bioactivation. Iran. J. Mater. Sci. Eng **2012,** *9* (3), 33-39. URL: http://ijmse.iust.ac.ir/article-1-174-en.html
7. Ghavidel, M.; Rabiee, S.; Rajabi, M. Engineering, THE EFFECT OF NANO BIOGLASS ON THE FABRICATION OF POROUS TITANIUM SCAFFOLDS. Iran. J. Mater. Sci. Eng **2014,** *11* (1), 62-66. URL: http://ijmse.iust.ac.ir/article-1-631-en.html
8. Jones, J. R. Reprint of: Review of bioactive glass: From Hench to hybrids. Acta Biomater **2015,** *23*, S53-S82. DOI: 10.1016/j.actbio.2015.07.019.
9. DUCHEYNE, P. Bioceramics: material characteristics versus in vivo behavior. J. Biomed. Mater. Res **1987,** *21* (A2), 219-236.
10. Yaszemski, M. J.; Payne, R. G.; Hayes, W. C.; Langer, R.; Mikos, A. G. Evolution of bone transplantation: molecular, cellular and tissue strategies to engineer human bone. Biomaterials **1996,** *17* (2), 175-185. DOI: 10.1016/0142-9612(96)85762-0
11. Habal, M. B.; Reddi, A. H. Bone grafts and bone induction substitutes. Clin Plast Surg **1994,** *21* (4), 525-542.
12. Kuo, C. K.; Ma, P. X. Ionically crosslinked alginate hydrogels as scaffolds for tissue engineering: Part 1. Structure, gelation rate and mechanical properties. Biomaterials **2001,** *22* (6), 511-521. DOI: 10.1016/S0142-9612(00)00201-5
13. Ishihara, M. Glycotechnology, Photocrosslinkable chitosan hydrogel as a wound dressing and a biological adhesive. Trends glycosci glyc **2002,** *14* (80), 331-341. DOI: /10.4052/tigg.14.331
14. Bartold, P. M.; Xiao, Y.; Lyngstaadas, S. P.; Paine, M. L.; Snead, M. L. Principles and applications of cell delivery systems for periodontal regeneration. Periodontology **2006,** *41* (1), 123-135. DOI: 10.1111/j.1600-0757.2006.00156.x
15. Muzzarelli, R.; Baldassarre, V.; Conti, F.; Ferrara, P.; Biagini, G.; Gazzanelli, G.; Vasi, V. J. B., Biological activity of chitosan: ultrastructural study. Biomaterials **1988,** *9* (3), 247-252. DOI: 10.1016/0142-9612(88)90092-0

16. Muzzarelli, R. A.; Giacomelli, G. The blood anticoagulant activity of N-carboxymethylchitosan trisulfate. Carbohydr. Polym **1987,** *7* (2), 87-96. DOI: 10.1016/0144-8617(87)90051-8
17. Jayakumar, R.; Nwe, N.; Tokura, S.; Tamura, H. Sulfated chitin and chitosan as novel biomaterials. nt. J. Biol. Macromol **2007,** *40* (3), 175-181. DOI: 10.1016/j.ijbiomac.2006.06.021
18. Jayakumar, R.; Prabaharan, M.; Reis, R.; Mano, J. Graft copolymerized chitosan—present status and applications. Carbohydr. Polym **2005,** *62* (2), 142-158. DOI: 10.1016/j.carbpol.2005.07.017
19. Nagahama, H.; Maeda, H.; Kashiki, T.; Jayakumar, R.; Furuike, T.; Tamura, H. Preparation and characterization of novel chitosan/gelatin membranes using chitosan hydrogel. Carbohydr. Polym **2009,** *76* (2), 255-260. DOI: 10.1016/j.carbpol.2008.10.015
20. Vacanti, J. P.; Langer, R. Tissue engineering: the design and fabrication of living replacement devices for surgical reconstruction and transplantation. The lancet **1999,** *354*, S32-S34. DOI: doi.org/10.1016/S0140-6736(99)90247-7
21. VandeVord, P. J.; Matthew, H. W.; DeSilva, S. P.; Mayton, L.; Wu, B.; Wooley, P. H. Evaluation of the biocompatibility of a chitosan scaffold in mice. J. Biomed. Mater. Res. A **2002,** *59* (3), 585-590. DOI: /10.1002/jbm.1270
22. Afewerki, S.; Sheikhi, A.; Kannan, S.; Ahadian, S.; Khademhosseini, A. Gelatin-polysaccharide composite scaffolds for 3D cell culture and tissue engineering: Towards natural therapeutics. bioengineering transla med **2019,** *4* (1), 96-115. DOI: 10.1002/btm2.10124
23. Loessner, D.; Meinert, C.; Kaemmerer, E.; Martine, L. C.; Yue, K.; Levett, P. A.; Klein, T. J.; Melchels, F. P.; Khademhosseini, A.; Hutmacher, D. W. Functionalization, preparation and use of cell-laden gelatin methacryloyl–based hydrogels as modular tissue culture platforms. Nature protocols **2016,** *11* (4), 727. DOI: 10.1038/nprot.2016.037
24. Byambaa, B.; Annabi, N.; Yue, K.; Trujillo-de Santiago, G.; Alvarez, M. M.; Jia, W.; Kazemzadeh-Narbat, M.; Shin, S. R.; Tamayol, A.; Khademhosseini, A. Bioprinted osteogenic and vasculogenic patterns for engineering 3D bone tissue. Adv. Healthc. Mater. **2017,** *6* (16), 1700015. DOI: 10.1002/adhm.201700015
25. Van Vlierberghe, S.; Dubruel, P.; Schacht, E. Biopolymer-based hydrogels as scaffolds for tissue engineering applications: a review. Biomacromolecules **2011,** *12* (5), 1387-1408. DOI: 10.1021/bm200083n
26. Jaipan, P.; Nguyen, A.; Narayan, R. J. Gelatin-based hydrogels for biomedical applications. MRS Commun **2017,** *7* (3), 416-426. DOI: 10.1557/mrc.2017.92
27. Mao, J. S.; Zhao, L. G.; Yin, Y. J.; De Yao, K. Structure and properties of bilayer chitosan–gelatin scaffolds. Biomaterials **2003,** *24* (6), 1067-1074. DOI: 10.1016/S0142-9612(02)00442-8
28. Chen, T.; Embree, H. D.; Brown, E. M.; Taylor, M. M.; Payne, G. F. Enzyme-catalyzed gel formation of gelatin and chitosan: potential for in situ applications. Biomaterials **2003,** *24* (17), 2831-2841. DOI: 10.1016/S0142-9612(03)00096-6
29. Mao, J.; Zhao, L.; De Yao, K.; Shang, Q.; Yang, G.; Cao, Y. Study of novel chitosan-gelatin artificial skin in vitro. Biomed Mater Res A **2003,** *64* (2), 301-308. DOI: 10.1002/jbm.a.10223

30. Xia, W.; Liu, W.; Cui, L.; Liu, Y.; Zhong, W.; Liu, D.; Wu, J.; Chua, K.; Cao, Y. Tissue engineering of cartilage with the use of chitosan-gelatin complex scaffolds. Appl. Bio Mater. **2004,** *71* (2), 373-380. DOI: 10.1002/jbm.b.30087
31. Yin, Y.; Ye, F.; Cui, J.; Zhang, F.; Li, X.; Yao, K. Preparation and characterization of macroporous chitosan–gelatin/β-tricalcium phosphate composite scaffolds for bone tissue engineering. J. Biomed. Mater. Res A **2003,** *67* (3), 844-855. DOI: 10.1002/jbm.a.10153
32. Shalumon, K.; Sowmya, S.; Sathish, D.; Chennazhi, K.; Nair, S. V.; Jayakumar, R. Effect of incorporation of nanoscale bioactive glass and hydroxyapatite in PCL/chitosan nanofibers for bone and periodontal tissue engineering. J. Biomed. Nanotechnol. **2013,** *9* (3), 430-440. DOI: 10.1166/jbn.2013.1559
33. Gentile, P.; Mattioli-Belmonte, M.; Chiono, V.; Ferretti, C.; Baino, F.; Tonda-Turo, C.; Vitale-Brovarone, C.; Pashkuleva, I.; Reis, R. L.; Ciardelli, G. Bioactive glass/polymer composite scaffolds mimicking bone tissue. J. Biomed. Mater. Res A **2012,** *100* (10), 2654-2667. DOI: 10.1002/jbm.a.34205
34. Peter, M.; Binulal, N.; Soumya, S.; Nair, S.; Furuike, T.; Tamura, H.; Jayakumar, R. Nanocomposite scaffolds of bioactive glass ceramic nanoparticles disseminated chitosan matrix for tissue engineering applications. Carbohydr. Polym **2010,** *79* (2), 284-289. DOI: 10.1016/j.carbpol.2009.08.001
35. Peter, M.; Binulal, N.; Nair, S.; Selvamurugan, N.; Tamura, H.; Jayakumar, R. Novel biodegradable chitosan–gelatin/nano-bioactive glass ceramic composite scaffolds for alveolar bone tissue engineering. Carbohydr. Polym **2010,** *158* (2), 353-361.
36. Bielby, R. C.; Pryce, R. S.; Hench, L. L.; Polak, J. M. Enhanced derivation of osteogenic cells from murine embryonic stem cells after treatment with ionic dissolution products of 58S bioactive sol–gel glass. Tissue Eng **2005,** *11* (3-4), 479-488.
37. Li, H.; Du, R.; Chang, J. Fabrication, characterization, and in vitro degradation of composite scaffolds based on PHBV and bioactive glass. J. Biomater. Appl **2005,** *20* (2), 137-155. DOI: 10.1016/j.cej.2010.02.003
38. Maji, K.; Dasgupta, S.; Pramanik, K.; Bissoyi, A. J. I. Preparation and evaluation of gelatin-chitosan-nanobioglass 3D porous scaffold for bone tissue engineering. Int. J. Biomater **2016,** *2016*. DOI: 10.1155/2016/9825659
39. Sohrabi, M.; Hesaraki, S.; Kazemzadeh, A. The influence of polymeric component of bioactive glass-based nanocomposite paste on its rheological behaviors and in vitro responses: Hyaluronic acid versus sodium alginate. J. Biomed Mater Res B Appl Biomater **2014,** *102* (3), 561-573. DOI: 10.1002/jbm.b.33035
40. Sohrabi, M.; Hesaraki, S.; Kazemzadeh, A.; Alizadeh, M. Development of injectable biocomposites from hyaluronic acid and bioactive glass nano-particles obtained from different sol–gel routes. Mater. Sci. Eng. C **2013,** *33* (7), 3730-3744. DOI: 10.1016/j.msec.2013.05.005
41. Kokubo, T.; Kushitani, H.; Sakka, S.; Kitsugi, T.; Yamamuro, T. Solutions able to reproduce in vivo surface-structure changes in bioactive glass-ceramic A-W3. J. Biomed. Mater. Res **1990,** *24* (6), 721-734. DOI: 10.1002/jbm.820240607
42. Lei, Y.; Rai, B.; Ho, K.; Teoh, S. In vitro degradation of novel bioactive polycaprolactone—20% tricalcium phosphate composite scaffolds for bone engineering. Mater. Sci. Eng. C **2007,** *27* (2), 293-298. DOI: 10.1016/j.msec.2006.05.006

43. Sohrabi, M.; Eftekhari Yekta, B.; Rezaie, H. R.; Naimi-Jamal, M. R. Rheology, injectability, and bioactivity of bioactive glass containing chitosan/gelatin, nano pastes. . Appl. Polym. Sci **2020,** *137* (41), 49240. DOI: 10.1002/app.49240
44. Sorrentino, R.; Cochis, A.; Azzimonti, B.; Caravaca, C.; Chevalier, J.; Kuntz, M.; Porporati, A. A.; Streicher, R. M.; Rimondini, L. Reduced bacterial adhesion on ceramics used for arthroplasty applications. J. Eur. Ceram. Soc **2018,** *38* (3), 963-970. DOI: 10.1016/j.jeurceramsoc.2017.10.008
45. Ferraris, S.; Cochis, A.; Cazzola, M.; Tortello, M.; Scalia, A.; Spriano, S.; Rimondini, L. biotechnology, Cytocompatible and anti-bacterial adhesion nanotextured titanium oxide layer on titanium surfaces for dental and orthopedic implants. Front. Bioeng. Biotechnol **2019,** *7*, 103. DOI: 10.3389/fbioe.2019.00103
46. Cochis, A.; Ferraris, S.; Sorrentino, R.; Azzimonti, B.; Novara, C.; Geobaldo, F.; Giachet, F. T.; Vineis, C.; Varesano, A.; Abdelgeliel, A. S. Silver-doped keratin nanofibers preserve a titanium surface from biofilm contamination and favor soft-tissue healing. J Mater Chem B. **2017,** *5* (42), 8366-8377. DOI: 10.1039/C7TB01965C
47. Bonifacio, M. A.; Cometa, S.; Cochis, A.; Gentile, P.; Ferreira, A. M.; Azzimonti, B.; Procino, G.; Ceci, E.; Rimondini, L.; De Giglio, E. Antibacterial effectiveness meets improved mechanical properties: Manuka honey/gellan gum composite hydrogels for cartilage repair. Carbohydr. Polym **2018,** *198*, 462-472. DOI: 10.1016/j.carbpol.2018.06.115
48. Bonifacio, M. A.; Cochis, A.; Cometa, S.; Scalzone, A.; Gentile, P.; Procino, G.; Milano, S.; Scalia, A. C.; Rimondini, L.; De Giglio, E. Advances in cartilage repair: the influence of inorganic clays to improve mechanical and healing properties of antibacterial Gellan gum-Manuka honey hydrogels. Mater. Sci. Eng. C **2020,** *108*, 110444. DOI: 10.1016/j.msec.2019.110444
49. Vernè, E.; Ferraris, S.; Vitale-Brovarone, C.; Cochis, A.; Rimondini, L. Bioactive glass functionalized with alkaline phosphatase stimulates bone extracellular matrix deposition and calcification in vitro. Appl. Surf. Sci **2014,** *313*, 372-381. DOI: 10.1016/j.apsusc.2014.06.001
50. Hill, R. An alternative view of the degradation of bioglass. J. Mater. Sci. Lett **1996,** *15* (13), 1122-1125.
51. Sohrabi, M.; Hesaraki, S.; Kazemzadeh, A. *Injectable bioactive glass/polysaccharide polymers nanocomposites for bone substitution*, Key Eng. Mater **2014**; pp 41-46. DOI: 10.4028/www.scientific.net/KEM.614.41
52. Hench, L. L. Bioceramics: from concept to clinic. J. Am. Ceram. Soc **1991,** *74* (7), 1487-1510. DOI: 10.1111/j.1151-2916.1991.tb07132.x
53. Li, X.; Xie, J.; Yuan, X.; Xia, Y. Coating electrospun poly (ε-caprolactone) fibers with gelatin and calcium phosphate and their use as biomimetic scaffolds for bone tissue engineering. Langmuir **2008,** *24* (24), 14145-14150. DOI: 10.1021/la802984a
54. Katsanevakis, E.; Wen, X. J.; Shi, D. L.; Zhang, N. In *Biomineralization of polymer scaffolds*, Key Eng. Mater **2010;** pp 269-295. DOI: 10.4028/www.scientific.net/KEM.441.269
55. Shirosaki, Y.; Tsuru, K.; Hayakawa, S.; Osaka, A.; Lopes, M. A.; Santos, J. D.; Costa, M. A.; Fernandes, M. H. Physical, chemical and in vitro biological profile of chitosan hybrid membrane as a function of organosiloxane concentration. Acta Biomater **2009,** *5* (1), 346-355. DOI: 10.1016/j.actbio.2008.07.022

56. Ren, L.; Tsuru, K.; Hayakawa, S.; Osaka, A. Synthesis and characterization of gelatin-siloxane hybrids derived through sol-gel procedure. J. Sol-gel Sci. Technol **2001,** *21* (1-2), 115-121. DOI: 10.1023/A:1011226104173
57. Chao, A.-C. Preparation of porous chitosan/GPTMS hybrid membrane and its application in affinity sorption for tyrosinase purification with Agaricus bisporus. J. Membr. Sci **2008,** *311* (1-2), 306-318. DOI: 10.1016/j.memsci.2007.12.032
58. Ravarian, R.; Craft, M.; Dehghani, F. Enhancing the biological activity of chitosan and controlling the degradation by nanoscale interaction with bioglass. J. Biomed Mater Res A **2015,** *103* (9), 2898-2908. DOI: 10.1002/jbm.a.35423
59. Lehtonen, T. J.; Tuominen, J. U.; Hiekkanen, E. Resorbable composites with bioresorbable glass fibers for load-bearing applications. In vitro degradation and degradation mechanism. Acta Biomater **2013,** *9* (1), 4868-4877. DOI: /10.1016/j.actbio.2012.08.052
60. Deschaseaux, F.; Pontikoglou, C.; Sensébé, L. medicine, m., Bone regeneration: the stem/progenitor cells point of view. J. Cell Mol Med **2010,** *14* (1-2), 103-115. DOI: 10.1111/j.1582-4934.2009.00878.x
61. Koob, S.; Torio-Padron, N.; Stark, G. B.; Hannig, C.; Stankovic, Z.; Finkenzeller, G. Bone formation and neovascularization mediated by mesenchymal stem cells and endothelial cells in critical-sized calvarial defects. Tissue Eng. Part A **2011,** *17* (3-4), 311-321. DOI: 10.1089/ten.tea.2010.0338
62. Li, M.; Liu, X.; Liu, X.; Ge, Calcium phosphate cement with BMP-2-loaded gelatin microspheres enhances bone healing in osteoporosis: a pilot study. Clin Orthop Relat Res **2010,** *468* (7), 1978-1985. DOI: 10.1007/s11999-010-1321-9
63. Mokhtari, H.; Ghasemi, Z.; Kharaziha, M.; Karimzadeh, F.; Alihosseini, F. Chitosan-58S bioactive glass nanocomposite coatings on TiO2 nanotube: Structural and biological properties. Appl. Surf. Sci **2018,** *441*, 138-149. DOI: /10.1016/j.apsusc.2018.01.314
64. Panjwani, B.; Sinha, S. K. Tribology and hydrophobicity of a biocompatible GPTMS/PFPE coating on Ti6Al4V surfaces. J Mech Behav Biomed Mater **2012,** *15*, 103-111. DOI: 10.1016/j.jmbbm.2012.06.016
65. Nájera-Romero, G. V.; Yar, M.; Rehman, I. U. Heparinized Chitosan/hydroxyapatite Scaffolds Stimulate Angiogenesis in CAM Assay: Future Proangiogenic Materials to Promote Neovascularization to Accelerate Bone Regeneration. Research Square **2020**. Doi: 10.21203/rs.3.rs-53262/v1
66. Wilcock, C.; Stafford, G.; Miller, C.; Ryabenkova, Y.; Fatima, M.; Gentile, P.; Möbus, G.; Hatton, P. Preparation and antibacterial properties of silver-doped nanoscale hydroxyapatite pastes for bone repair and augmentation. J. Biomed. Nanotechnol **2017,** *13* (9), 1168-1176. DOI: 10.1166/jbn.2017.2387
67. Fei Liu, X.; Lin Guan, Y.; Zhi Yang, D.; Li, Z.; De Yao, K. Antibacterial action of chitosan and carboxymethylated chitosan. J. Appl. Polym. Sci **2001,** *79* (7), 1324-1335. DOI: 10.1002/1097-4628(20010214)79:7<1324::AID-APP210>3.0.CO;2-L
68. da Silva, B. L.; Caetano, B. L.; Chiari-Andréo, B. G.; Pietro, R. C. L. R.; Chiavacci, L. A. Increased antibacterial activity of ZnO nanoparticles: influence of size and surface modification. Colloids Surf. B **2019,** *177*, 440-447. DOI: 10.1016/j.colsurfb.2019.02.013
69. Gafri, H. F. S.; Zuki, F. M.; Aroua, M. K.; Hashim, N. A. Mechanism of bacterial adhesion on ultrafiltration membrane modified by natural antimicrobial polymers (chitosan) and

combination with activated carbon (PAC). Rev. Chem. Eng **2019,** *35* (3), 421-443. DOI: 10.1515/revce-2017-0006

70. Tharanathan, R. technology, Biodegradable films and composite coatings: past, present and future. Trends Food Sci Tech **2003,** *14* (3), 71-78. DOI: 10.1016/S0924-2244(02)00280-7
71. Lin, W.-H.; Yu, J.; Chen, G.; Tsai, W.-B. Biointerfaces, S. B., Fabrication of multi-biofunctional gelatin-based electrospun fibrous scaffolds for enhancement of osteogenesis of mesenchymal stem cells. Colloids and Surfaces B: Biointerfaces **2016,** *138*, 26-31. DOI: 10.1016/j.colsurfb.2015.11.017
72. Wu, I.-T.; Kao, P.-F.; Huang, Y.-R.; Ding, S.-J. In vitro and in vivo osteogenesis of gelatin-modified calcium silicate cement with washout resistance. Mater. Sci. Eng. C **2020,** *117*, 111297. DOI: 10.1016/j.msec.2020.111297
73. Ren, K.; Wang, Y.; Sun, T.; Yue, W.; Zhang, H. Electrospun PCL/gelatin composite nanofiber structures for effective guided bone regeneration membranes. Mater. Sci. Eng. C **2017,** *78*, 324-332. DOI: 10.1016/j.msec.2017.04.084
74. Gao, G.; Schilling, A. F.; Yonezawa, T.; Wang, J.; Dai, G.; Cui, X. Bioactive nanoparticles stimulate bone tissue formation in bioprinted three-dimensional scaffold and human mesenchymal stem cells. Biotechnol. J **2014,** *9* (10), 1304-1311. DOI: 10.1002/biot.201400305
75. Hoppe, A.; Güldal, N. S.; Boccaccini, A. R. A review of the biological response to ionic dissolution products from bioactive glasses and glass-ceramics. Biomaterials **2011,** *32* (11), 2757-2774. DOI: 10.1016/j.biomaterials.2011.01.004